

# Aerodynamic Coefficient Prediction Technique for Finned Missiles at High Incidence

William B. Baker Jr.\*

ARO, Inc., Arnold Air Force Station, Tenn.

An aerodynamic coefficient prediction technique, based on a high angle-of-attack data base, is presented for the calculation of normal-force and pitching-moment coefficients for slender bodies with low-aspect-ratio fins at angles of attack up to 180 deg. Comparisons are made between predicted coefficients and data from the high angle-of-attack data base. Also, comparisons are made between predicted coefficients and independent data. Tables and graphs are available to allow hand calculation of coefficients for other configurations at selected Mach numbers and angles of attack.

## Nomenclature

$R$	= exposed aspect ratio = $b^2 / (2S_f)$	$X_{CPBFH}$	= distance from hinge line to effective center of pressure of body on fin interference, non-dimensionalized by $C_R$
$b$	= fin exposed span, in.	$X_{CPBOF}$	= distance from moment reference to effective center of pressure of body on fin interference, calibers
$b'$	= total span of fins plus body, in.	$X_{CPFA}$	= distance from moment reference to fin alone center of pressure, calibers
$C_{dc}$	= crossflow drag coefficient	$X_{CPFOB}$	= distance from moment reference to effective center of pressure of fin on body interference, calibers
$C_m$	= pitching moment coefficient	$X_{HL}$	= distance from moment reference to hinge line, negative aft of moment reference, calibers
$C_{mBA}$	= body alone pitching moment coefficient	$X_m$	= distance from actual nose to moment reference, calibers
$C_{mH}$	= hinge-moment coefficient	$Y_{CPBOF}$	= distance from root chord to effective center of pressure of body on fin interference, non-dimensionalized by $b/2$
$C_{mRB}$	= root bending-moment coefficient	$Z$	= empirical correlation to body alone pitching moment coefficient
$C_N$	= normal-force coefficient	$Z_{max}$	= maximum value of empirical pitching moment correction
$C_{NBA}$	= body alone normal force coefficient	$\alpha$	= angle of attack
$C_{NFA}$	= fin alone normal force coefficient	$\beta_0$	= regression coefficient (intercept)
$C_{NFB}$	= fin in presence of body normal force coefficient	$\beta_1$	= regression coefficient ( $\lambda$ )
$CP_{XHLA}$	= fin alone center of pressure measured in $X$ direction from hinge line, nondimensionalized by $C_R$	$\beta_2$	= regression coefficient ( $\lambda^2$ )
$CP_{XHLB}$	= fin in presence of body center of pressure measured in $X$ direction from hinge line, non-dimensionalized by $C_R$	$\beta_3$	= regression coefficient ( $R$ )
$CP_{YRCA}$	= fin alone center of pressure measured in $Y$ direction from root chord, nondimensionalized by $b/2$	$\beta_4$	= regression coefficient ( $d/b'$ )
$C_R$	= root chord, in.	$\Delta C_{NBOF}$	= incremental normal force due to body on fin interference
$C_T$	= tip chord, in.	$\Delta C_{NFOB}$	= incremental normal force due to fin on body interference
$d$	= body diameter, reference length, in.	$\delta$	= normalized body alone pitching moment correction
$d/b'$	= span ratio	$\eta$	= ratio of crossflow drag of a circular cylinder of finite length to one of infinite length
$l$	= total configuration length, in.	$\eta'$	= ratio of crossflow drag of a circular cylinder of finite length to one of infinite length, corrected for Mach number
$M$	= Mach number	$\lambda$	= taper ratio of fin ( $C_T/C_R$ )
$M_c$	= crossflow Mach number		
$Re_c$	= crossflow Reynolds number		
$S$	= cross-sectional area of body, reference area, in. <sup>2</sup>		
$S_b$	= area of base, in. <sup>2</sup>		
$S_f$	= exposed area of one fin, in. <sup>2</sup>		
$S_p$	= total planform area, in. <sup>2</sup>		
$V$	= total volume, in. <sup>3</sup>		
$\bar{X}$	= centroid of total plan area, measured from actual nose, in.		
$X_{CP}$	= distance from moment reference to center of pressure, calibers		
$X_{CPBA}$	= distance from moment reference to body alone center of pressure, calibers		

Presented as Paper 78-60 at the AIAA 16th Aerospace Sciences Meeting, Huntsville, Ala., Jan. 16-18, 1978; submitted Jan. 23, 1978; revision received May 22, 1978. Copyright © American Institute of Aeronautics and Astronautics, Inc., 1978. All rights reserved.

Index categories: LV/M Aerodynamics; LV/M Configurational Design.

\*Research Engineer, 4T Projects Branch, Propulsion Wind Tunnel Facility, AEDC Division. Associate Fellow AIAA.

## Introduction

TO extend the state-of-the-art aerodynamic coefficient prediction methodology at high angles of attack, a semiempirical prediction technique has been developed for the prediction of normal-force and pitching-moment coefficients for slender-body-alone and slender-body-plus-fin configurations. Additionally, installed fin normal-force, root-bending, and hinge-moment coefficients are calculated. The semiempirical prediction technique is valid for slender bodies

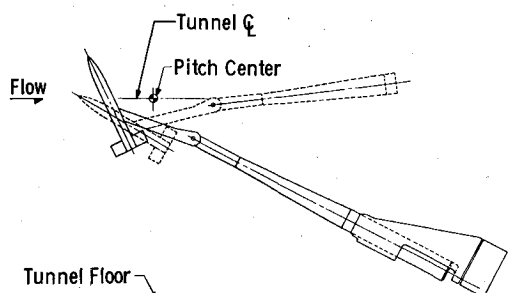


Fig. 1 Installation of  $l/d = 10$  slender body in tunnel 4T,  $\alpha = 0-90$  deg.

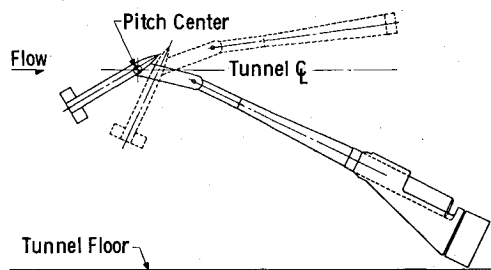


Fig. 2 Installation of  $l/d = 10$  slender body in tunnel 4T,  $\alpha = 90-180$  deg.

with low-aspect-ratio fins at Mach numbers from 0.6 to 3.0, angles of attack from 0 to 180 deg, and no rocket plume effects. The range of validity of the prediction technique for the low-aspect-ratio fins is for an aspect ratio from 0.5 to 2.0, a taper ratio from 0 to 1.0, and a span ratio from 0.3 to 0.5. Wind tunnel testing was accomplished at Mach numbers from 0.6 to 3.0 to provide the data base from which the prediction technique was derived. The data base provides the first parametric set of data at angles of attack from 0 to 180 deg. The data base will also provide a standard of comparison for high angle-of-attack prediction methodology developed in the future.

### Technical Discussion

A group of wind tunnel models was tested in the aerodynamic wind tunnel (4T) of the Propulsion Wind Tunnel Facility (PWT) and in the supersonic wind tunnel (A) of the von Karman Gas Dynamics Facility (VKF) at the Arnold Engineering Development Center (AEDC). Data were obtained with blunt base, strut-mounted, ogive-cylinder models (Figs. 1 and 2) tested both with and without fins. Data were also obtained with fin models mounted on a reflection plane (Fig. 3) to provide fin-alone data at high angles of attack. The total forces and moments on the models as well as the forces and moments on the fin in the presence of the body were measured, thus providing body-alone, body-plus-fin, and installed-fin loads at high angles of attack. The tests are described in detail in Ref. 1.

With the high angle-of-attack data set it was possible to develop a semiempirical, high angle-of-attack, aerodynamic coefficient prediction technique. A detailed description of the prediction technique is also given in Ref. 1; however, a brief description of the technique follows. The forces and their centers of pressure acting on the finned slender body are shown in Fig. 4.

It is assumed in the development of this prediction technique that the total normal-force coefficient for a slender body with four fins arranged in a cruciform-plus orientation is made up of the body-alone normal force  $C_{N_{BA}}$  and the fin-alone normal force  $C_{N_{FA}}$ , combined with the incremental normal force attributable to the interference of the fin on the body  $\Delta C_{N_{FOB}}$  and the incremental normal force attributable to the interference of the body on the fin  $\Delta C_{N_{BOF}}$ . A linear

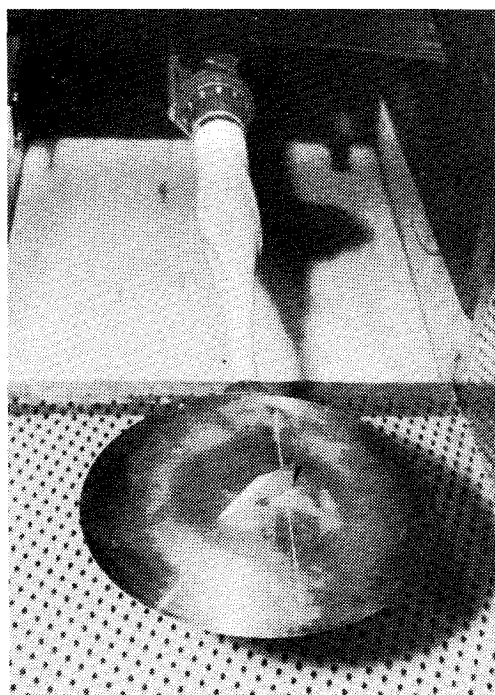


Fig. 3 Installation of reflection plane.

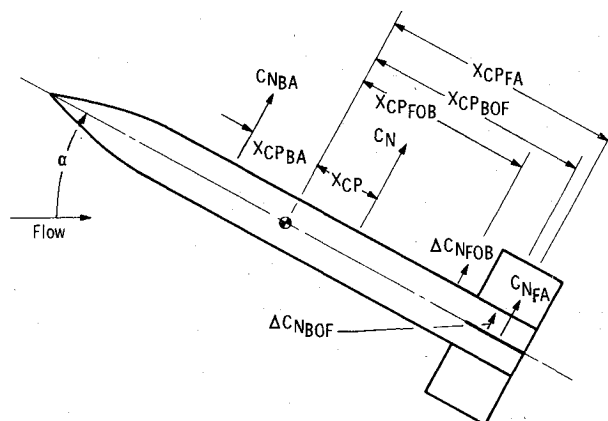


Fig. 4 Forces and their centers of pressure on finned slender body.

combination of the contributions of each component is given by

$$C_N = C_{N_{BA}} + 2(C_{N_{FA}})(S_f/S) + \Delta C_{N_{FOB}}(S_f/S) + 2(\Delta C_{N_{BOF}})(S_f/S) \quad (1)$$

where each component is converted to a common reference area. The pitching-moment coefficient is likewise assumed to be a linear combination of the force contributions along with their centers of pressure or effective centers of pressure. The pitching-moment equation for the slender body with four fins is given by

$$C_m = C_{m_{BA}} + 2(C_{N_{FA}})(X_{CP_{FA}})(S_f/S) + (\Delta C_{N_{FOB}})(X_{CP_{FOB}})(S_f/S) + 2(\Delta C_{N_{BOF}})(X_{CP_{BOF}})(S_f/S) \quad (2)$$

where  $X_{CP_{FOB}}$  and  $X_{CP_{BOF}}$  are the effective centers of pressure of the incremental forces attributable to interference. Center-of-pressure locations in the moment equation are nondimensionalized by  $d$ . The development of the calculation procedure is now established.

### Body-Alone Method

This part of the procedure calculates the forces and moments for slender finless bodies at angles of attack to 180 deg. The method is based on a modification of the crossflow theory formulated by Jorgensen.<sup>2</sup> The crossflow drag coefficient variation with Mach number and Reynolds number is a modification of the variation reported by Fidler and Bateman<sup>3</sup> and the variation used in the USAF Datcom.<sup>4</sup> The equation for normal-force coefficient for the range  $0 \leq \alpha \leq 180$  deg is given by

$$C_{N_{BA}} = (S_b/S) \sin(2\alpha') \cos(\alpha'/2) + \eta' C_{d_c} (S_p/S) \sin^2(\alpha') \quad (3)$$

The modified pitching-moment equation for the range  $0 \leq \alpha \leq 90$  deg is given by

$$C_{m_{BA}} = \left[ \frac{V - S_b(l - X_m)}{Sd} \right] \sin(2\alpha') \cos\left(\frac{\alpha'}{2}\right) + \eta' C_{d_c} \left( \frac{S_p}{S} \right) \frac{(X_m - \bar{X})}{d} \sin^2(\alpha') + Z \quad (4)$$

and the pitching-moment equation for the range  $90 < \alpha \leq 180$  deg is given by

$$C_{m_{BA}} = - \left[ \frac{V - S_b X_m}{Sd} \right] \sin(2\alpha') \cos\left(\frac{\alpha'}{2}\right) + \eta' C_{d_c} \left( \frac{S_p}{S} \right) \left[ \frac{(X_m - \bar{X})}{d} \right] \sin^2(\alpha') + Z \quad (5)$$

where

$$\alpha' = \alpha \quad (0 \leq \alpha \leq 90 \text{ deg}) \quad (6a)$$

$$\alpha' = 180 - \alpha \quad (90 < \alpha \leq 180 \text{ deg}) \quad (6b)$$

The location of the aerodynamic center given by

$$X_{CP_{BA}} = C_{m_{BA}} / C_{N_{BA}} \quad (7)$$

is measured from the moment reference location specified by  $X_m$  and is positive forward of the moment reference point.

The term  $\eta'$  is used to modify the two-dimensional drag coefficient to approximate the drag coefficient for a finite length cylinder and is determined from the data obtained by Goldstein,<sup>5</sup> corrected for Mach number in the range  $0.95 \leq M \leq 1.35$ . The variation of  $\eta$  as a function of length-to-diameter ratio of the cylinder, shown in Fig. 5, was obtained by a least-squares, fifth-order polynomial curve fit approximating Goldstein's  $\eta$  curve.<sup>5</sup> It has been customary in the past to assume that the finite length correction applied only at subsonic Mach numbers. At Mach numbers of 1.0 or greater, the term was constant and equal to 1.0. This assumption causes a discontinuous change in the normal force and pitching moment at a Mach number of 1.0. However, since there is a mixture of both subsonic and supersonic flow over the body at high subsonic Mach numbers, a rapid but smooth change in  $\eta$  would be the most likely variation. Also, the discontinuous change in  $\eta$  at  $M=1.0$  results in an overprediction of  $C_N$  at  $M=1.0$  and  $\alpha=90$  deg. Therefore, a hyperbolic tangent variation in  $\eta$  over the region  $0.95 \leq M \leq 1.35$  has been assumed in the development of this technique. The variation of  $\eta$  with  $l/d$  of the configuration is determined from Fig. 5 and then modified for Mach number in the range  $0.95 \leq M \leq 1.35$  by the following equation:

$$\eta' = \eta + [(1.0 - \eta)/2] \times [1.0 + \tanh\{(M - 1.0)(15.0/M^4)\}] \quad (8)$$

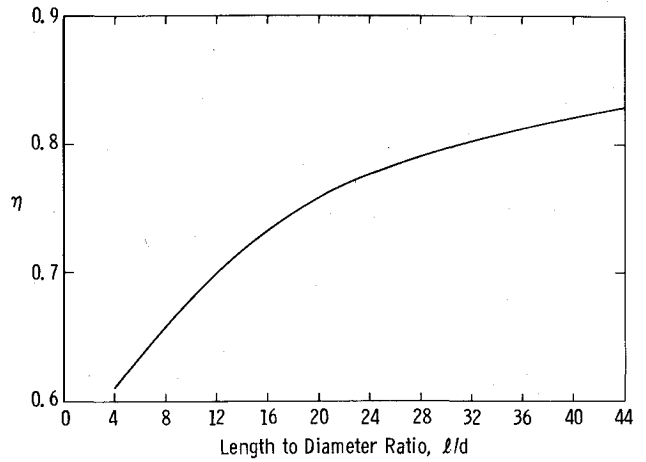


Fig. 5 Finite length cylinder correction.

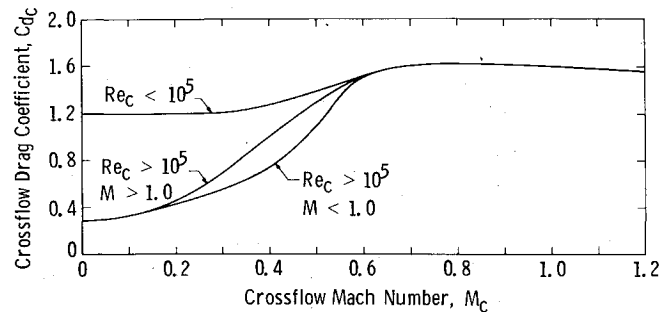


Fig. 6 Crossflow drag coefficient.

The fourth power of the Mach number in the last term allows for a rapid increase in the region  $0.95 \leq M \leq 1.0$  with a slower increase in  $\eta'$  in the region  $1.0 < M \leq 1.35$ .

The crossflow drag coefficient  $C_{d_c}$ , used in this procedure, is shown in Fig. 6 as a function of crossflow Mach number, freestream Mach number, and crossflow Reynolds number. For a crossflow Mach number up to 0.6, the crossflow drag variation was taken from Ref. 3. At higher crossflow Mach numbers, the crossflow drag is assumed to be a function of crossflow Mach number only and is represented by a modification of the crossflow drag from the U.S. Air Force Datcom.<sup>4</sup>

The term  $Z$ , which appears in the pitching-moment equation, is the empirical modification to the crossflow theory to make the theory fit the observed data from the high angle-of-attack data base. The term is a function of both Mach number and angle of attack.  $Z$  was determined by subtracting the pitching-moment coefficient calculated by Jorgensen's formulation of the crossflow theory from the measured pitching-moment coefficient:

$$Z = C_{m_{meas}} - C_{m_{calc}} \quad (9)$$

For each Mach number,  $Z$ , as a function of angle of attack, was normalized by its extremum value. The resulting  $\delta$  is shown in Fig. 7 for each Mach number. A curve,  $\delta$  (weighted toward  $M=0.9$ ), also shown in Fig. 7, represents the assumed variation of  $\delta$  with angle of attack. The normalizing factor  $Z_{max}$  is shown in Fig. 8 as a function of Mach number.

Another empirical factor based on experimental data obtained for bodies with  $l/d$  of 12 and 15,<sup>1</sup> was added to account for a body with  $(l/d)$  different from the data used to determine the correction. Thus, the resulting factor is given by

$$Z = (Z_{max}) (\delta) \left( \frac{l/d}{10} \right)^2 \quad (10)$$

### Interference Factors

The incremental interference force coefficients  $\Delta C_{N_{FOB}}$  and  $\Delta C_{N_{BOF}}$ , or interference factors, along with their effective

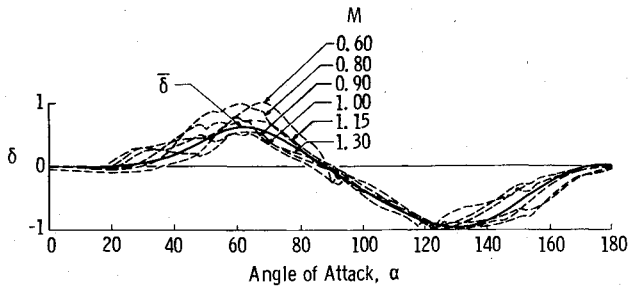


Fig. 7 Nondimensional body-alone pitching-moment coefficient correction.

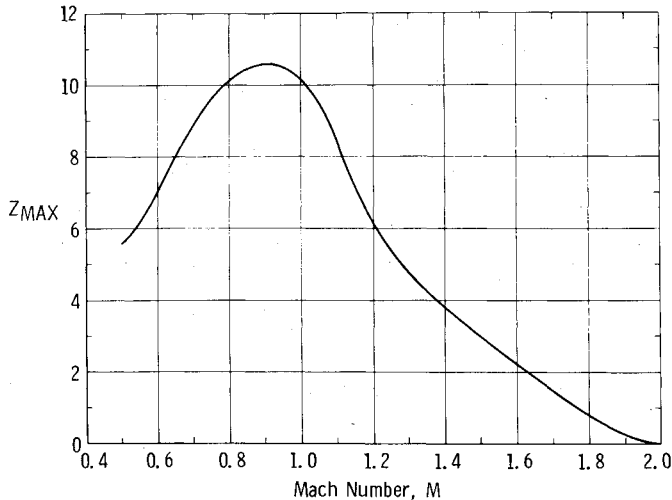


Fig. 8 Mach number variation of maximum value of body-alone pitching-moment coefficient correction.

centers of pressure were determined from the data in the high angle-of-attack data set. Only the data obtained for the  $l/d=10$  total length configuration were used to empirically determine the interference factors.

The incremental normal-force coefficient on the fin attributable to the presence of the body was determined by subtracting the normal-force coefficient measured on the fins alone from the normal-force coefficient measured on the fins in the presence of the body:

$$\Delta C_{N_{BOF}} = C_{N_{FB}} - C_{N_{FA}} \quad (11)$$

This interference factor has a reference area based on the fin area and will be converted to a reference area based on body cross-sectional area in the final normal-force and pitching-moment equations.

The incremental interference normal-force coefficient on the body attributable to the presence of the fin can now be determined by rearranging the assumed equation for the total normal-force coefficient, Eq. (1).

$$\Delta C_{N_{FOB}} = [C_N - C_{N_{BA}} - 2(C_{N_{FA}})(S_f/S) - 2(\Delta C_{N_{BOF}})(S_f/S)](S/S_f) \quad (12)$$

Again, this interference is based on fin area and will be converted in the final equation. Now with the two interference factors known, their effective centers of pressure must be determined. The effective center of pressure in the  $X$  direction relative to the fin hingeline can be determined for the interference factor  $\Delta C_{N_{BOF}}$  by using the measured fin hinge moment for the cases of the fin alone and the fin in the presence of the body. The interference hinge moment is obtained by subtracting the hinge moment measured on the fins alone from the hinge moment measured on the fins in the

presence of the body. The following equation is given for the interference hinge moment:

$$\begin{aligned} &(\Delta C_{N_{BOF}})(X_{CP_{BFH}}) \\ &= (C_{N_{FB}})(CP_{X_{HLB}}) - (C_{N_{FA}})(CP_{X_{HLA}}) \end{aligned} \quad (13)$$

resulting in

$$X_{CP_{BFH}} = \frac{C_{N_{FB}} CP_{X_{HLB}} - C_{N_{FA}} CP_{X_{HLA}}}{\Delta C_{N_{BOF}}} \quad (14)$$

The lateral effective center of pressure  $Y_{CP_{BOF}}$  can be determined in a like manner from the measured fin-alone and installed-fin root bending moments. Center-of-pressure locations in the hinge moment equation are nondimensionalized by  $C_R$ , and center-of-pressure locations associated with the root bending moments are nondimensionalized by  $b/2$ .

The effective center of pressure of the interference is related to the hinge line and is nondimensionalized by the root chord length. It must now be determined relative to the center of gravity of the configuration and nondimensionalized by the body diameter for use in the final pitching-moment equation. The hinge line location  $X_{HL}$  relative to the center of gravity for finned bodies, is an input parameter and is negative aft of the center of gravity. It follows that

$$X_{CP_{BOF}} = X_{HL} + X_{CP_{BFH}}(C_R/d) \quad (15)$$

The effective center of pressure of the interference factor  $\Delta C_{N_{FOB}}$  can now be determined by rearranging the equation for the total pitching-moment coefficient, Eq. (2):

$$\begin{aligned} X_{CP_{FOB}} = & \\ \frac{C_m - C_{m_{BA}} - 2\Delta C_{N_{BOF}}(S_f/S)X_{CP_{BOF}} - 2C_{N_{FA}}X_{CP_{FA}}(S_f/S)}{\Delta C_{N_{FOB}}(S_f/S)} \end{aligned} \quad (16)$$

where

$$X_{CP_{FA}} = X_{HL} + CP_{X_{HLA}}(C_R/d) \quad (17)$$

By the nature of the equation, the effective center of pressure  $X_{CP_{BOF}}$  is nondimensionalized by the body diameter.

The interference factors and their effective centers of pressure have been mathematically represented by a hyper-surface determined at each Mach number and angle of attack, using a multiple linear regression technique. The dependent variable on the surface is represented as a function of the three ratios – taper, aspect, and span – which define the fin.

#### Fin-Alone Method

The fin-alone contribution to the normal-force coefficient and total pitching-moment coefficient is determined by a surface fit to the measured data at each angle of attack and Mach number. The surface was determined in a manner similar to the interference factors by the multiple linear regression technique. The fin-alone variables of fin normal force  $C_{N_{FA}}$ , center-of-pressure location in the  $X$  direction  $CP_{X_{HLA}}$ , and center-of-pressure location in the  $Y$  direction  $CP_{Y_{RCA}}$  are determined at each Mach number and angle of attack by an equation which is a function of the two ratios, taper and aspect, which are independent of the body and define the fin.

#### Multiple Linear Regression Technique

The multiple linear regression technique, used to represent the calculated interference factors and the measured fin-alone

data by surface equations is a standard application program,<sup>6</sup> and the following equations result:

$$\Delta C_{N_{FOB}} = \beta_0 + \beta_1 \lambda + \beta_2 \lambda^2 + \beta_3 R + \beta_4 (d/b') \quad (18a)$$

$$\Delta C_{N_{BOF}} = \beta_0 + \beta_1 \lambda + \beta_2 \lambda^2 + \beta_3 R + \beta_4 (d/b') \quad (18b)$$

$$X_{CP_{FOB}} = \beta_0 + \beta_1 \lambda + \beta_2 \lambda^2 + \beta_3 R + \beta_4 (d/b') \quad (18c)$$

$$Y_{CP_{BOF}} = \beta_0 + \beta_1 \lambda + \beta_2 \lambda^2 + \beta_3 R + \beta_4 (d/b') \quad (18d)$$

$$X_{CP_{BFH}} = \beta_0 + \beta_1 \lambda + \beta_2 \lambda^2 + \beta_3 R + \beta_4 (d/b') \quad (18e)$$

$$C_{N_{FA}} = \beta_0 + \beta_1 \lambda + \beta_2 \lambda^2 + \beta_3 R \quad (18f)$$

$$CP_{X_{HLA}} = \beta_0 + \beta_1 \lambda + \beta_2 \lambda^2 + \beta_3 R \quad (18g)$$

$$CP_{Y_{RCA}} = \beta_0 + \beta_1 \lambda + \beta_2 \lambda^2 + \beta_3 R \quad (18h)$$

A unique set of regression coefficients,  $\beta_0$  to  $\beta_4$  or  $\beta_0$  to  $\beta_3$ , is tabulated in Ref. 7 for each of the foregoing parameters. The coefficients are given for angles of attack from 0 to 180 deg in 2-deg increments and for 10 Mach numbers ranging from 0.6 to 3.0.

#### Calculation Procedure

For a given finned slender body, the total normal-force and pitching-moment coefficients are given by Eqs. (1) and (2), respectively. Each component of the two equations is determined separately. The body-alone normal force is determined by Eqs. (4) and (5). The factors  $C_{d_n}$  and  $\eta$  are determined from Figs. 6 and 5, respectively, with  $\eta'$  determined by Eq. (8). The factor  $Z$  is determined from Eq. (10) with  $\delta$  and  $Z_{\max}$  determined from Figs. 7 and 8, respectively.

The interference factors and their effective centers of pressure are determined from the regression coefficients,  $\beta_0 \dots \beta_4$ , tabulated in Ref. 7 and the first five of Eqs. (18). The fin-alone contributions are determined by the regression coefficients,  $\beta_0 \dots \beta_3$ , tabulated in Ref. 7 and the last three of

Eqs. (18). The fin parameters are determined from the following equations:

$$C_{N_{FB}} = C_{N_{FA}} + \Delta C_{N_{BOF}} \quad (19)$$

$$C_{m_H} = (C_{N_{FA}})(CP_{X_{HLA}}) + (\Delta C_{N_{BOF}})(X_{CP_{BFH}}) \quad (20)$$

$$C_{m_{RB}} = (C_{N_{FA}})(CP_{Y_{RCA}}) + (\Delta C_{N_{BOF}})(Y_{CP_{BOF}}) \quad (21)$$

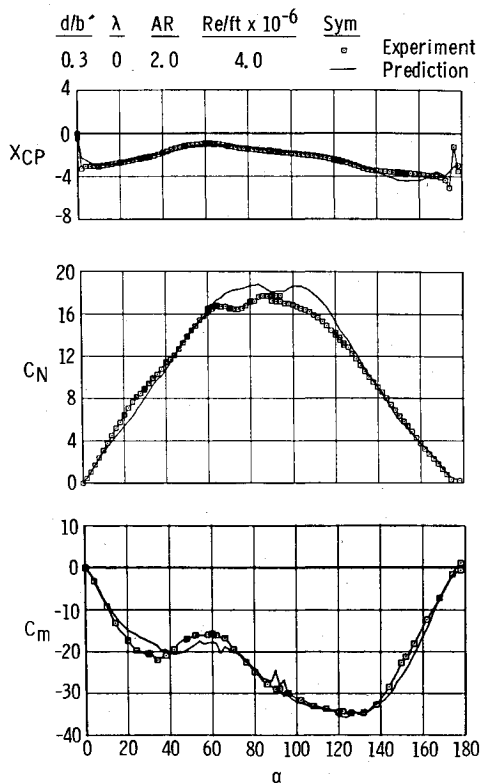


Fig. 9 Comparison of measured and predicted force and moment coefficients for ogive cylinder with triangular tail fins,  $M=0.8$ .

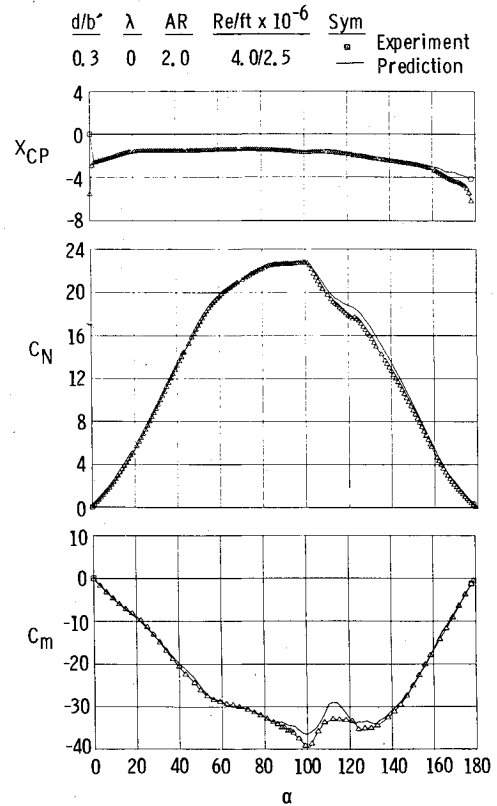


Fig. 10 Comparison of measured and predicted force and moment coefficients for ogive cylinder with triangular tail fins,  $M=2.0$ .

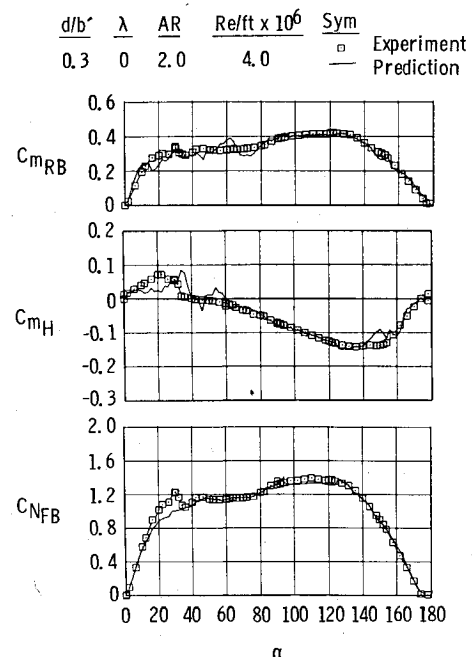


Fig. 11 Comparison of measured and predicted fin loads for a triangular fin on an ogive cylinder,  $M=0.8$ .

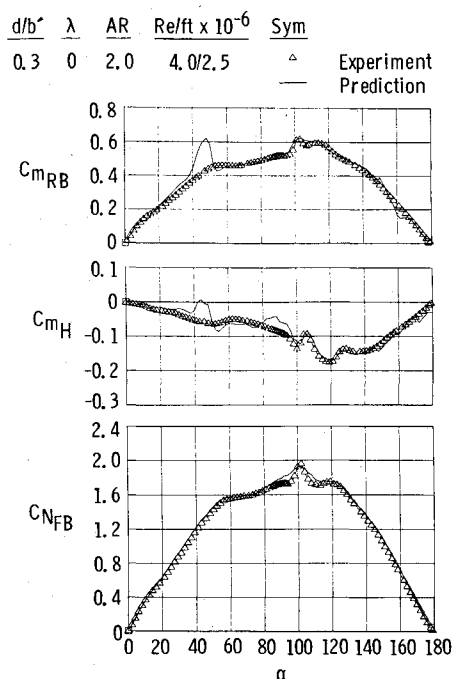


Fig. 12 Comparison of measured and predicted fin loads for a triangular fin on an ogive cylinder,  $M=2.0$ .

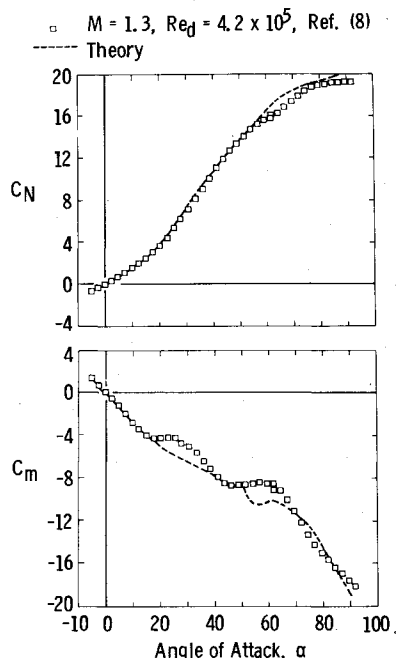


Fig. 13 Comparison of measured and predicted coefficients for a modified basic finner model having an ogive-cylinder body and low-aspect-ratio fins.

Since the regression coefficients are determined for discrete Mach numbers and angles of attack, values for other Mach numbers and angles of attack must be determined by interpolation. A computer version of the coefficient prediction technique has been written for the IBM 370/165 computer and is described in detail in Ref. 7.

### Comparisons with Data

A comparison of the measured and predicted normal force and pitching moment at Mach numbers of 0.8 and 2.0 is shown in Figs. 9 and 10, where the symbol size approximates the experimental uncertainty, for an ogive-cylinder configuration from the high angle-of-attack data set, 10 calibers long with an aspect ratio 2, triangular fin. Figures 11 and 12 show a comparison of measured and predicted fin loads for the preceding configuration. As can be seen in Figs. 9-12, the agreement between the measured and predicted coefficients is excellent.

The only high angle-of-attack data for a slender body with low-aspect-ratio fins at transonic Mach numbers other than the data in the high angle-of-attack data base are reported by Jenke.<sup>8</sup> The comparison of the measured and predicted aerodynamic coefficients is shown in Fig. 13 at a Mach number of 1.3. The model had a roll rate of approximately 100 rad/s for the data shown. The measured and predicted values of normal force and pitching moment are seen to be in excellent agreement.

### Conclusions

A high angle-of-attack data set has been established, and a semiempirical theory, adequate for preliminary design purposes, has been developed for the prediction of aerodynamic coefficients for finned slender bodies at angles of attack from 0 to 180 deg and Mach numbers from 0.6 to 3.0.

### Acknowledgments

The work reported herein was conducted by the Arnold Engineering Development Center (AEDC), Air Force Systems Command (AFSC) for the Air Force Flight Dynamics Lab (FGC). Research and analysis work was done by personnel of ARO, Inc., a Sverdrup Corporation Company, operating contractor of AEDC. Further reproduction is authorized to satisfy needs of the U.S. Government.

### References

- <sup>1</sup>Baker, W. B., "An Aerodynamic Coefficient Prediction Technique for Slender Bodies with Low Aspect Ratio Fins at Transonic Mach Numbers and Angles of Attack to 180 Degrees," Ph.D. Dissertation, University of Tennessee, Aug. 1976.
- <sup>2</sup>Jorgensen, L. H., "Prediction of Static Aerodynamic Characteristics for Space-Shuttle-Like, and Other Bodies at Angles of Attack from 0° to 180°," NASA TN D6996, Jan. 1973.
- <sup>3</sup>Fidler, J. E. and Bateman, M. C., "Aerodynamic Methodology (Isolated Fins and Bodies)," U.S. Army Missile Command, USAMC-OR 12, 399, March 1973.
- <sup>4</sup>Finck, R. D., "USAF Stability and Control DATCOM," McDonnell Douglas Corporation, Douglas Aircraft Division, Oct. 1960; revised Jan. 1975.
- <sup>5</sup>Goldstein, S., *Modern Developments in Fluid Dynamics*, Oxford University Press, 1938.
- <sup>6</sup>IBM Application Program, "System/360 Scientific Subroutine Package, Version III, Programmers Manual, Program Number (360A-CM-03X)," 5th Ed., GH20-0205-4, Aug. 1970.
- <sup>7</sup>Baker, W. B., "An Aerodynamic Coefficient Prediction Technique for Slender Bodies with Low Aspect Ratio Fins at Mach Numbers from 0.6 to 3.0 and Angles of Attack from 0 to 180 Degrees," Arnold Engineering Development Center, Arnold Air Force Station, Tenn., AEDC-TR-77-97, March 1978.
- <sup>8</sup>Jenke, L. M., "Experimental Roll-Damping, Magnus and Static-Stability Characteristics of Two Slender Missile Configurations at High Angles of Attack (0-90 Deg) and Mach Numbers 0.2 through 2.5," Arnold Engineering Development Center, Arnold Air Force Station, Tenn., AEDC-TR-76-58 (AD-A027027), 1976.